WHERE ARE WE NOW?
STATE OF THE ART AND FUTURE TRENDS OF SOLVERS FOR HARD ARGUMENTATION PROBLEMS

Federico Cerutti[†] · Mauro Vallati[*] · Massimiliano Giacomin[+]

xv · ix · mmxvi

[†]Cardiff University · [*] University of Huddersfield · [+]Università degli Studi di Brescia

Definition

An *argumentation framework* (AF) is a pair $\Gamma = \langle \mathcal{A}, \mathcal{R} \rangle$ where $\mathcal{A}$ is a set of arguments and $\mathcal{R} \subseteq \mathcal{A} \times \mathcal{A}$. We say that $\mathbf{b}$ *attacks* $\mathbf{a}$ iff $\langle \mathbf{b}, \mathbf{a} \rangle \in \mathcal{R}$, also denoted as $\mathbf{b} \to \mathbf{a}$.

Definition

Given an AF $\Gamma = \langle \mathcal{A}, \mathcal{R} \rangle$:

- a set S $\subseteq \mathcal{A}$ is a *conflict–free* set of Γ if $\nexists\, \mathbf{a}, \mathbf{b} \in$ S s.t. $\mathbf{a} \rightarrow \mathbf{b}$;
- an argument $\mathbf{a} \in \mathcal{A}$ is *acceptable* with respect to a set S $\subseteq \mathcal{A}$ of Γ if $\forall \mathbf{b} \in \mathcal{A}$ s.t. $\mathbf{b} \rightarrow \mathbf{a}$, $\exists\, \mathbf{c} \in$ S s.t. $\mathbf{c} \rightarrow \mathbf{b}$;
- a set S $\subseteq \mathcal{A}$ is an *admissible set* of Γ if S is a conflict–free set of Γ and every element of S is acceptable with respect to S of Γ.

Definition

Given an AF $\Gamma = \langle \mathcal{A}, \mathcal{R} \rangle$: a set S $\subseteq \mathcal{A}$ is a:

- *preferred extension* of Γ iff S is a maximal (w.r.t. set inclusion) admissible set of Γ;
- *stable extension* of Γ iff S is a conflict–free set of Γ and $\mathcal{A} \setminus \text{S} = \{\mathbf{a} \in \mathcal{A} \mid \mathbf{b} \rightarrow \mathbf{a} \text{ and } \mathbf{b} \in \text{S}\}$.

Summary Report of the First International Competition on Computational Models of Argumentation

Matthias Thimm, Serena Villata, Federico Cerutti, Nir Oren, Hannes Strass, Mauro Vallati

■ *We review the First International Competition on Computational Models of Argumentation (ICCMA'15). The competition evaluated submitted solvers' performance on four different computational tasks related to solving abstract argumentation frameworks. Each task evaluated solvers in ways that pushed the edge of existing performance by introducing new challenges. Despite being the first competition in this area, the high number of competitors entered, and differences in results, suggest that the competition will help shape the landscape of ongoing developments in argumentation theory solvers.*

Computational models of argumentation are an active research discipline within artificial intelligence that has grown since the beginning of the 1990s (Dung 1995). While still a young field when compared to areas such as SAT solving and logic programming, the argumentation community is very active, with a conference series (COMMA, which began in 2006) and a variety of workshops and special issues of journals. Argumentation has also worked its way into a variety of applications. For example, Williams et al. (2015) described how argumentation techniques are used for recommending cancer treatments, while Toniolo et al. (2015) detail how argumentation-based techniques can support critical thinking and collaborative scientific inquiry or intelligence analysis.

Many of the problems that argumentation deals with are computationally difficult, and applications utilizing argumentation therefore require efficient solvers. To encourage this line of research, we organised the First International Competition on Computational Models of Argumentation (ICCMA), with the intention of assessing and promoting state-of-the-art solvers for abstract argumentation problems, and to identify families of challenging benchmarks for such solvers.

  ISSN 0738-4602

First Impression:
Reduction-based systems are the most efficient

ICCMA15 RESULTS

EE-PR

1. Cegartix
2. ArgSemSAT
3. CoQuiAAS
4. ASPARTIX-V
5. LabSATSolver
6. prefMaxSAT
7. ASGL
8. ASPARTIX-D
9. ConArg
10. ArgTools
11. ...

EE-ST

1. ASPARTIX-D
2. ArgSemSAT
3. CoQuiAAS
4. ASGL
5. ConArg
6. ArgTools
7. LabSATSolver
8. DIAMOND
9. Dungell
   Carneades
   ASSA

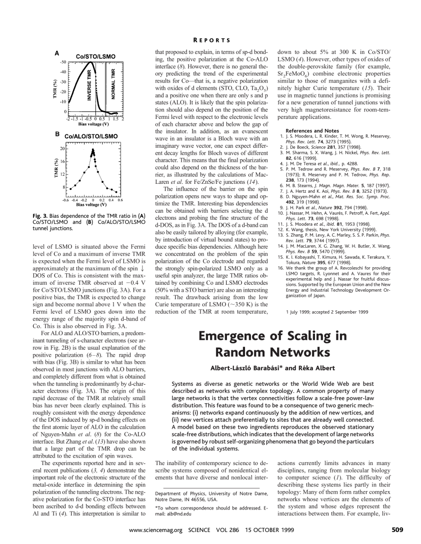

Fig. 3. Bias dependence of the TMR ratio in (**A**) Co/STO/LSMO and (**B**) Co/ALO/STO/LSMO tunnel junctions.

level of LSMO is situated above the Fermi level of Co and a maximum of inverse TMR is expected when the Fermi level of LSMO is approximately at the maximum of the spin ↓ DOS of Co. This is consistent with the maximum of inverse TMR observed at −0.4 V for Co/STO/LSMO junctions (Fig. 3A). For a positive bias, the TMR is expected to change sign and become normal above 1 V when the Fermi level of LSMO goes down into the energy range of the majority spin d-band of Co. This is also observed in Fig. 3A.

For ALO and ALO/STO barriers, a predominant tunneling of s-character electrons (see arrow in Fig. 2B) is the usual explanation of the positive polarization (*6–8*). The rapid drop with bias (Fig. 3B) is similar to what has been observed in most junctions with ALO barriers, and completely different from what is obtained when the tunneling is predominantly by d-character electrons (Fig. 3A). The origin of this rapid decrease of the TMR at relatively small bias has never been clearly explained. This is roughly consistent with the energy dependence of the DOS induced by sp-d bonding effects on the first atomic layer of ALO in the calculation of Nguyen-Mahn *et al*. (*8*) for the Co-ALO interface. But Zhang *et al*. (*13*) have also shown that a large part of the TMR drop can be attributed to the excitation of spin waves.

The experiments reported here and in several recent publications (*3, 4*) demonstrate the important role of the electronic structure of the metal-oxide interface in determining the spin polarization of the tunneling electrons. The negative polarization for the Co-STO interface has been ascribed to d-d bonding effects between Al and Ti (*4*). This interpretation is similar to that proposed to explain, in terms of sp-d bonding, the positive polarization at the Co-ALO interface (*8*). However, there is no general theory predicting the trend of the experimental results for Co—that is, a negative polarization with oxides of d elements (STO, CLO, Ta_2O_5) and a positive one when there are only s and p states (ALO). It is likely that the spin polarization should also depend on the position of the Fermi level with respect to the electronic levels of each character above and below the gap of the insulator. In addition, as an evanescent wave in an insulator is a Bloch wave with an imaginary wave vector, one can expect different decay lengths for Bloch waves of different character. This means that the final polarization could also depend on the thickness of the barrier, as illustrated by the calculations of MacLaren *et al*. for Fe/ZnSe/Fe junctions (*14*).

The influence of the barrier on the spin polarization opens new ways to shape and optimize the TMR. Interesting bias dependencies can be obtained with barriers selecting the d electrons and probing the fine structure of the d-DOS, as in Fig. 3A. The DOS of a d-band can also be easily tailored by alloying (for example, by introduction of virtual bound states) to produce specific bias dependencies. Although here we concentrated on the problem of the spin polarization of the Co electrode and regarded the strongly spin-polarized LSMO only as a useful spin analyzer, the large TMR ratios obtained by combining Co and LSMO electrodes (50% with a STO barrier) are also an interesting result. The drawback arising from the low Curie temperature of LSMO (~350 K) is the reduction of the TMR at room temperature, down to about 5% at 300 K in Co/STO/LSMO (*4*). However, other types of oxides of the double-perovskite family (for example, Sr_2FeMoO_6) combine electronic properties similar to those of manganites with a definitely higher Curie temperature (*15*). Their use in magnetic tunnel junctions is promising for a new generation of tunnel junctions with very high magnetoresistance for room-temperature applications.

References and Notes

1. J. S. Moodera, L. R. Kinder, T. M. Wong, R. Meservey, *Phys. Rev. Lett.* **74**, 3273 (1995).
2. J. De Boeck, *Science* **281**, 357 (1998).
3. M. Sharma, S. X. Wang, J. H. Nickel, *Phys. Rev. Lett.* **82**, 616 (1999).
4. J. M. De Teresa *et al., ibid.*, p. 4288.
5. P. M. Tedrow and R. Meservey, *Phys. Rev. B* **7**, 318 (1973); R. Meservey and P. M. Tedrow, *Phys. Rep.* **238**, 173 (1994).
6. M. B. Stearns, *J. Magn. Magn. Mater.* **5**, 187 (1997).
7. J. A. Hertz and K. Aoi, *Phys. Rev. B* **8**, 3252 (1973).
8. D. Nguyen-Mahn *et al., Mat. Res. Soc. Symp. Proc.* **492**, 319 (1998).
9. J. H. Park *et al., Nature* **392**, 794 (1998).
10. J. Nassar, M. Hehn, A. Vaurès, F. Petroff, A. Fert, *Appl. Phys. Lett.* **73**, 698 (1998).
11. J. S. Moodera *et al., ibid.* **81**, 1953 (1998).
12. K. Wang, thesis, New York University (1999).
13. S. Zhang, P. M. Levy, A. C. Marley, S. S. P. Parkin, *Phys. Rev. Lett.* **79**, 3744 (1997).
14. J. M. MacLaren, X. G. Zhang, W. H. Butler, X. Wang, *Phys. Rev. B* **59**, 5470 (1999).
15. K. I. Kobayashi, T. Kimura, H. Sawada, K. Terakura, Y. Tokura, *Nature* **395**, 677 (1998).
16. We thank the group of A. Revcoleschi for providing LSMO targets, R. Lyonnet and A. Vaures for their experimental help and J. Nassar for fruitful discussions. Supported by the European Union and the New Energy and Industrial Technology Development Organization of Japan.

1 July 1999; accepted 2 September 1999

Emergence of Scaling in Random Networks

Albert-László Barabási* and Réka Albert

Systems as diverse as genetic networks or the World Wide Web are best described as networks with complex topology. A common property of many large networks is that the vertex connectivities follow a scale-free power-law distribution. This feature was found to be a consequence of two generic mechanisms: (i) networks expand continuously by the addition of new vertices, and (ii) new vertices attach preferentially to sites that are already well connected. A model based on these two ingredients reproduces the observed stationary scale-free distributions, which indicates that the development of large networks is governed by robust self-organizing phenomena that go beyond the particulars of the individual systems.

The inability of contemporary science to describe systems composed of nonidentical elements that have diverse and nonlocal interactions currently limits advances in many disciplines, ranging from molecular biology to computer science (*1*). The difficulty of describing these systems lies partly in their topology: Many of them form rather complex networks whose vertices are the elements of the system and whose edges represent the interactions between them. For example, liv-

Department of Physics, University of Notre Dame, Notre Dame, IN 46556, USA.

*To whom correspondence should be addressed. E-mail: alb@nd.edu

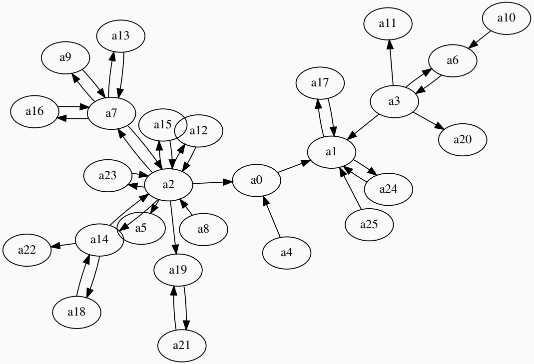

On random graphs I.

Dedicated to O. Varga, at the occasion of his 50th birthday.

By P. ERDÖS and A. RÉNYI (Budapest).

Let us consider a "random graph" $\Gamma_{n,N}$ having n possible (labelled) vertices and N edges; in other words, let us choose at random (with equal probabilities) one of the $\binom{\binom{n}{2}}{N}$ possible graphs which can be formed from the n (labelled) vertices $P_1, P_2, \ldots, P_n$ by selecting N edges from the $\binom{n}{2}$ possible edges $\overline{P_iP_j}$ $(1 \leqq i < j \leqq n)$. Thus the effective number of vertices of $\Gamma_{n,N}$ may be less than n, as some points P_i may be not connected in $\Gamma_{n,N}$ with any other point P_j; we shall call such points P_i *isolated* points. We consider the isolated points also as belonging to $\Gamma_{n,N}$. $\Gamma_{n,N}$ is called completely connected if it effectively contains all points $P_1, P_2, \ldots, P_n$ (i. e. if it has no isolated points) and is connected in the ordinary sense. In the present paper we consider asymptotic statistical properties of random graphs for $n \to +\infty$. We shall deal with the following questions:

1. What is the probability of $\Gamma_{n,N}$ being completely connected?

2. What is the probability that the greatest connected component (subgraph) of $\Gamma_{n,N}$ should have effectively $n-k$ points? $(k=0, 1, \ldots)$.

3. What is the probability that $\Gamma_{n,N}$ should consist of exactly $k+1$ connected components? $(k=0, 1, \ldots)$.

4. If the edges of a graph with n vertices are chosen successively so that after each step every edge which has not yet been chosen has the same probability to be chosen as the next, and if we continue this process until the graph becomes completely connected, what is the probability that the number of necessary steps ν will be equal to a given number l?

As (partial) answers to the above questions we prove the following four theorems. In Theorems 1, 2, and 3 we use the notation

$$N_c = \left[\frac{1}{2} n \log n + cn\right] \tag{1}$$

where c is an arbitrary fixed real number ($[x]$ denotes the integer part of x).

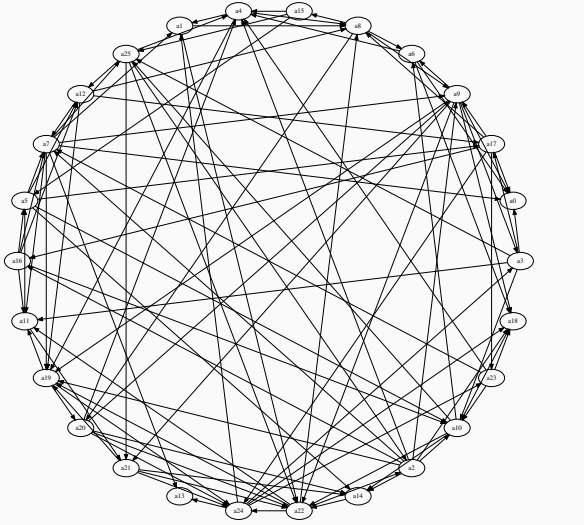

probo / Code / [r45

https://sourcefc

```
17  import java.util.concurrent.Executors;
18  import java.util.concurrent.Future;
19  import java.util.concurrent.TimeUnit;
20  import java.util.concurrent.TimeoutException;
21
22  import net.sf.probo.writer.ApxWriter;
23  import net.sf.probo.writer.TgfWriter;
24  import net.sf.probo.writer.Writer;
25  import net.sf.tweety.arg.dung.CompleteReasoner;
26  import net.sf.tweety.arg.dung.DungTheory;
27  import net.sf.tweety.arg.dung.GroundReasoner;
28  import net.sf.tweety.arg.dung.PreferredReasoner;
29  import net.sf.tweety.arg.dung.StableReasoner;
30  import net.sf.tweety.arg.dung.semantics.Extension;
31  import net.sf.tweety.arg.dung.syntax.Argument;
32  import net.sf.tweety.arg.dung.syntax.Attack;
33  import net.sf.tweety.commons.util.RandomSubsetIterator;
34  import net.sf.tweety.commons.util.SubsetIterator;
35  import net.sf.tweety.logics.pl.sat.LingelingSolver;
36  import net.sf.tweety.logics.pl.sat.SatSolver;
37
38
39  /**
40   * This is the generator for abstract argumentation graphs used
41   * in ICCMA'15 for the second group of problems (testcases 4-6). It generates
42   * graphs that (likely) possess many stable, preferred, and complete extension
43   * It works roughly as follows:
44   * 1.) A set of arguments is identified to form an acyclic subgraph, containin
45   *  the likely grounded extension
46   * 2.) a subset of arguments is randomly selected and attacks are randomly add
47   *   from some arguments within this set to all arguments outside the set (exc
48   *   to the arguments identified in 1.)
49   * 3.) Step 2 is repeated until a number of desired stable extensions is reach
50   * For more details see the code.
51   *
52   * This generator can be used by adapting the variables in the configuration b
53   * beginning of the class. Once started, this generator generates graphs conti
54   * (it will not terminate on its own, the application has to be terminated for
55   *
56   * @author Matthias Thimm
57   */
58  public class StableGenerator {
59
```

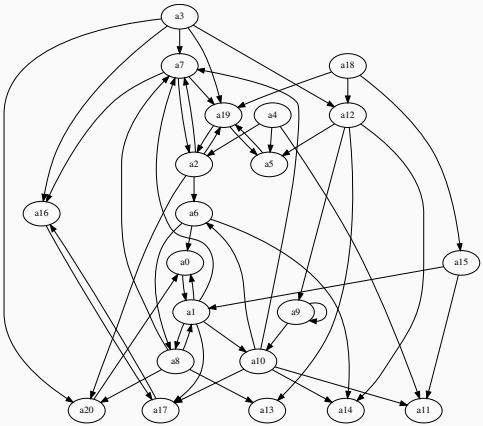

typically slower than $\sim 1\,km\,s^{-1}$) might differ significantly from what is assumed by current modelling efforts[27]. The expected equation-of-state differences among small bodies (ice versus rock, for instance) presents another dimension of study; having recently adapted our code for massively parallel architectures (K. M. Olson and E.A, manuscript in preparation), we are now ready to perform a more comprehensive analysis.

The exploratory simulations presented here suggest that when a young, non-porous asteroid (if such exist) suffers extensive impact damage, the resulting fracture pattern largely defines the asteroid's response to future impacts. The stochastic nature of collisions implies that small asteroid interiors may be as diverse as their shapes and spin states. Detailed numerical simulations of impacts, using accurate shape models and rheologies, could shed light on how asteroid collisional response depends on internal configuration and shape, and hence on how planetesimals evolve. Detailed simulations are also required before one can predict the quantitative effects of nuclear explosions on Earth-crossing comets and asteroids, either for hazard mitigation[28] through disruption and deflection, or for resource exploitation[29]. Such predictions would require detailed reconnaissance concerning the composition and internal structure of the targeted object. □

Received 4 February; accepted 18 March 1998.

1. Asphaug, E. & Melosh, H. J. The Stickney impact of Phobos: A dynamical model. *Icarus* **101,** 144–164 (1993).
2. Asphaug, E. *et al*. Mechanical and geological effects of impact cratering on Ida. *Icarus* **120,** 158–184 (1996).
3. Nolan, M. C., Asphaug, E., Melosh, H. J. & Greenberg, R. Impact craters on asteroids: Does strength or gravity control their size? *Icarus* **124,** 359–371 (1996).
4. Love, S. J. & Ahrens, T. J. Catastrophic impacts on gravity dominated asteroids. *Icarus* **124,** 141–155 (1996).
5. Melosh, H. J. & Ryan, E. V. Asteroids: Shattered but not dispersed. *Icarus* **129,** 562–564 (1997).
6. Housen, K. R., Schmidt, R. M. & Holsapple, K. A. Crater ejecta scaling laws: Fundamental forms based on dimensional analysis. *J. Geophys. Res.* **88,** 2485–2499 (1983).
7. Holsapple, K. A. & Schmidt, R. M. Point source solutions and coupling parameters in cratering mechanics. *J. Geophys. Res.* **92,** 6350–6376 (1987).
8. Housen, K. R. & Holsapple, K. A. On the fragmentation of asteroids and planetary satellites. *Icarus* **84,** 226–253 (1990).
9. Benz, W. & Asphaug, E. Simulations of brittle solids using smooth particle hydrodynamics. *Comput. Phys. Commun.* **87,** 253–265 (1995).
10. Asphaug, E. *et al*. Mechanical and geological effects of impact cratering on Ida. *Icarus* **120,** 158–184 (1996).
11. Hudson, R. S. & Ostro, S. J. Shape of asteroid 4769 Castalia (1989 PB) from inversion of radar images. *Science* **263,** 940–943 (1994).
12. Ostro, S. J. *et al.* Asteroid radar astrometry. *Astron. J.* **102,** 1490–1502 (1991).
13. Ahrens, T. J. & O'Keefe, J. D. in *Impact and Explosion Cratering* (eds Roddy, D. J., Pepin, R. O. & Merrill, R. B.) 639–656 (Pergamon, New York, 1977).
14. Tillotson, J. H. Metallic equations of state for hypervelocity impact. (General Atomic Report GA-3216, San Diego, 1962).
15. Nakamura, A. & Fujiwara, A. Velocity distribution of fragments formed in a simulated collisional disruption. *Icarus* **92,** 132–146 (1991).
16. Benz, W. & Asphaug, E. Simulations of brittle solids using smooth particle hydrodynamics. *Comput. Phys. Commun.* **87,** 253–265 (1995).
17. Bottke, W. F., Nolan, M. C., Greenberg, R. & Kolvoord, R. A. Velocity distributions among colliding asteroids. *Icarus* **107,** 255–268 (1994).
18. Belton, M. J. S. *et al.* Galileo encounter with 951 Gaspra—First pictures of an asteroid. *Science* **257,** 1647–1652 (1992).
19. Belton, M. J. S. *et al.* Galileo's encounter with 243 Ida: An overview of the imaging experiment. *Icarus* **120,** 1–19 (1996).
20. Asphaug, E. & Melosh, H. J. The Stickney impact of Phobos: A dynamical model. *Icarus* **101,** 144–164 (1993).
21. Asphaug, E. *et al*. Mechanical and geological effects of impact cratering on Ida. *Icarus* **120,** 158–184 (1996).
22. Housen, K. R., Schmidt, R. M. & Holsapple, K. A. Crater ejecta scaling laws: Fundamental forms based on dimensional analysis. *J. Geophys. Res.* **88,** 2485–2499 (1983).
23. Veverka, J. *et al.* NEAR's flyby of 253 Mathilde: Images of a C asteroid. *Science* **278,** 2109–2112 (1997).
24. Asphaug, E. *et al*. Impact evolution of icy regoliths. *Lunar Planet. Sci. Conf. (Abstr.)* **XXVIII,** 63–64 (1997).
25. Love, S. G., Hörz, F. & Brownlee, D. E. Target porosity effects in impact cratering and collisional disruption. *Icarus* **105,** 216–224 (1993).
26. Fujiwara, A., Cerroni, P., Davis, D. R., Ryan, E. V. & DiMartino, M. in *Asteroids II* (eds Binzel, R. P., Gehrels, T. & Matthews, A. S.) 240–265 (Univ. Arizona Press, Tucson, 1989).
27. Davis, D. R. & Farinella, P. Collisional evolution of Edgeworth-Kuiper Belt objects. *Icarus* **125,** 50–60 (1997).
28. Ahrens, T. J. & Harris, A. W. Deflection and fragmentation of near-Earth asteroids. *Nature* **360,** 429–433 (1992).
29. *Resources of Near-Earth Space* (eds Lewis, J. S., Matthews, M. S. & Guerrieri, M. L.) (Univ. Arizona Press, Tucson, 1993).

Acknowledgements. This work was supported by NASA's Planetary Geology and Geophysics Program.

Correspondence and requests for materials should be addressed to E.A. (e-mail: asphaug@earthsci.ucsc.edu).

Collective dynamics of 'small-world' networks

Duncan J. Watts* & Steven H. Strogatz

Department of Theoretical and Applied Mechanics, Kimball Hall, Cornell University, Ithaca, New York 14853, USA

Networks of coupled dynamical systems have been used to model biological oscillators[1–4], Josephson junction arrays[5,6], excitable media[7], neural networks[8–10], spatial games[11], genetic control networks[12] and many other self-organizing systems. Ordinarily, the connection topology is assumed to be either completely regular or completely random. But many biological, technological and social networks lie somewhere between these two extremes. Here we explore simple models of networks that can be tuned through this middle ground: regular networks 'rewired' to introduce increasing amounts of disorder. We find that these systems can be highly clustered, like regular lattices, yet have small characteristic path lengths, like random graphs. We call them 'small-world' networks, by analogy with the small-world phenomenon[13,14] (popularly known as six degrees of separation[15]). The neural network of the worm *Caenorhabditis elegans*, the power grid of the western United States, and the collaboration graph of film actors are shown to be small-world networks. Models of dynamical systems with small-world coupling display enhanced signal-propagation speed, computational power, and synchronizability. In particular, infectious diseases spread more easily in small-world networks than in regular lattices.

To interpolate between regular and random networks, we consider the following random rewiring procedure (Fig. 1). Starting from a ring lattice with n vertices and k edges per vertex, we rewire each edge at random with probability p. This construction allows us to 'tune' the graph between regularity ($p = 0$) and disorder ($p = 1$), and thereby to probe the intermediate region $0 < p < 1$, about which little is known.

We quantify the structural properties of these graphs by their characteristic path length $L(p)$ and clustering coefficient $C(p)$, as defined in Fig. 2 legend. Here $L(p)$ measures the typical separation between two vertices in the graph (a global property), whereas $C(p)$ measures the cliquishness of a typical neighbourhood (a local property). The networks of interest to us have many vertices with sparse connections, but not so sparse that the graph is in danger of becoming disconnected. Specifically, we require $n \gg k \gg \ln(n) \gg 1$, where $k \gg \ln(n)$ guarantees that a random graph will be connected[16]. In this regime, we find that $L \sim n/2k \gg 1$ and $C \sim 3/4$ as $p \rightarrow 0$, while $L \approx L_{random} \sim \ln(n)/\ln(k)$ and $C \approx C_{random} \sim k/n \ll 1$ as $p \rightarrow 1$. Thus the regular lattice at $p = 0$ is a highly clustered, large world where L grows linearly with n, whereas the random network at $p = 1$ is a poorly clustered, small world where L grows only logarithmically with n. These limiting cases might lead one to suspect that large C is always associated with large L, and small C with small L.

On the contrary, Fig. 2 reveals that there is a broad interval of p over which $L(p)$ is almost as small as L_{random} yet $C(p) \gg C_{random}$. These small-world networks result from the immediate drop in $L(p)$ caused by the introduction of a few long-range edges. Such 'short cuts' connect vertices that would otherwise be much farther apart than L_{random}. For small p, each short cut has a highly nonlinear effect on L, contracting the distance not just between the pair of vertices that it connects, but between their immediate neighbourhoods, neighbourhoods of neighbourhoods and so on. By contrast, an edge

* Present address: Paul F. Lazarsfeld Center for the Social Sciences, Columbia University, 812 SIPA Building, 420 W118 St, New York, New York 10027, USA.

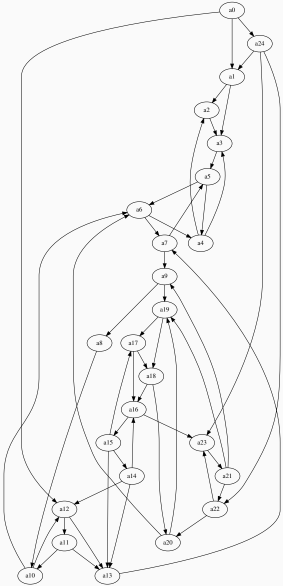

$$\text{PAR10}(s, P) = \begin{cases} 10 * T & \text{if P is unsolved} \\ t_P(s) & \text{otherwise} \end{cases}$$

T indicates the considered timeout
$t_P(s)$ denotes the time needed by solver s to solve problem P


7
6
5
4
3
2
1
UNITED
7
4

EE-PR											
	All			Barabasi-Albert		Erdös-Rényi		StableM		Watts-Strogatz	
Solver	PAR10	Cov.	F.t	PAR10	Cov.	PAR10	Cov.	PAR10	Cov.	PAR10	Cov.
Cegartix	**1350.4**	**79.1**	229	1662.6	74.2	1266.6	81.0	**1439.2**	**77.0**	1028.6	84.2
ArgSemSAT	1916.2	69.1	35	3532.3	41.9	433.7	94.2	2530.9	58.7	1171.1	81.5
LabSATSolver	2050.3	66.8	9	3430.7	43.5	261.3	96.5	2869.5	53.0	1657.5	73.9
prefMaxSAT	2057.2	66.8	273	3482.1	42.9	444.0	94.2	3625.2	40.3	**697.5**	**89.4**
DIAMOND	2417.0	61.0	1	3447.8	43.2	1366.7	79.0	2831.8	53.7	2026.0	68.0
ASPARTIX-D	2728.6	56.1	4	4101.5	32.6	3067.8	51.6	2068.8	66.7	1630.3	74.3
ASPARTIX-V	2772.2	55.2	21	3646.6	40.3	3292.6	47.1	2340.7	62.0	1772.4	71.9
CoQuiAas	3026.4	50.5	78	3736.1	38.4	2873.4	53.5	2836.4	53.3	2645.1	57.1
ASGL	3477.3	43.2	1	4809.7	20.3	96.1	**100.0**	4475.4	26.0	4585.5	25.4
Conarg	3696.3	39.3	158	1128.7	81.6	2813.9	55.8	4934.6	18.3	6000.0	0.0
ArgTools	3906.2	35.2	**322**	3694.4	39.0	**45.2**	**100.0**	6000.0	0.0	6000.0	0.0
GRIS	4543.7	24.4	174	**254.6**	**96.1**	6000.0	0.0	6000.0	0.0	6000.0	0.0

EE-ST											
	All			Barabasi-Albert		Erdös-Rényi		StableM		Watts-Strogatz	
Solver	PAR10	Cov.	F.t	PAR10	Cov.	PAR10	Cov.	PAR10	Cov.	PAR10	Cov.
ArgTools	440.7	94.5	245	1328.6	78.4	47.4	**100.0**	**144.1**	**100.0**	**230.5**	**100.0**
LabSATSolver	641.6	90.0	352	396.2	93.9	**22.7**	**100.0**	1497.6	76.0	684.9	90.7
ASPARTIX-D	829.7	87.1	**395**	412.2	93.5	1194.4	81.6	1187.2	81.0	535.0	93.0
CoQuiAas	1477.2	76.2	372	1453.3	76.5	1485.1	76.5	1879.0	69.3	1106.5	83.3
DIAMOND	1555.4	75.2	42	2527.1	58.7	692.2	89.7	1887.2	69.7	1127.1	83.7
ArgSemSAT	1826.6	70.5	70	4019.0	33.5	408.9	94.5	1970.0	68.0	900.8	87.0
Conarg	1976.4	67.8	292	**261.4**	**96.1**	33.6	**100.0**	3742.1	38.3	4010.0	35.3
ASGL	2647.6	57.3	11	2737.4	56.1	85.2	**100.0**	3723.8	38.7	4152.8	33.7

STATIC PORTFOLIOS

Defined by:

1. the selected solvers;
2. the order in which solvers will be run; and
3. the runtime allocated to each solver.

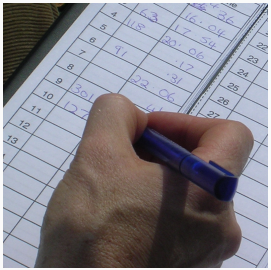

Shared-k

Each component solver has been allocated $\frac{\text{maxRuntime}}{k}$ seconds. Solvers selected/ordered according to overall PAR10

FDSS

From an empty portfolio, we iteratively add either a new solver component, or extend the allocated CPU-time of a solver already added to the portfolio, depending on what maximises the increment of the PAR10 score of the portfolio

PER-INSTANCE PORTFOLIOS

For each AF a vector of features is computed. Similar instances should have similar feature vectors. Portfolios are configured using empirical performance models

Classification-based

Classify

It classifies a given AF into a single category which corresponds to the single solver predicted to be the fastest and allocates it all the available CPU-time

Regression-based

1-Regression

Given the predicted runtime of each solver, the solver predicted to be the fastest is selected and it has allocated all the available CPU-time

M-regression

Initially we select the solver predicted to be the fastest, but we allocate only its predicted CPU-time +10%. If such a solver does not solve the given AF in the allocated time, it is stopped and no longer available to be selected, and the process iterates by selecting a different solver

VS.

EE-PR

System	Cov.	PAR10
VBS	91.4	562.9
Classify	89.7	665.2
1-Regression	88.6	734.7
M-Regression	82.8	1068.3
FDSS	80.0	1311.4
Cegartix	79.1	1350.4
Shared-2	73.2	1678.0
Shared-3	69.4	1892.0
ArgSemSAT	69.1	1916.2
LabSATSolver	66.8	2050.3
prefMaxSAT	66.8	2057.2
Shared-4	65.7	2105.5
Shared-5	63.3	2240.3
DIAMOND	61.0	2417.0
ASPARTIX-D	56.1	2728.6
ASPARTIX-V	55.2	2772.2
CoQuiAas	50.5	3026.4
ASGL	43.2	3477.3
Conarg	39.3	3696.3
ArgTools	35.2	3906.2
GRIS	24.4	4543.7

EE-ST

System	Cov.	PAR10
VBS	100.0	39.3
1-Regression	97.4	206.9
Classify	97.1	217.5
Shared-2	97.7	262.3
M-Regression	94.7	378.4
Shared-3	94.0	420.1
ArgTools	94.5	440.7
LabSATSolver	90.0	641.6
FDSS	89.4	677.4
ASPARTIX-D	87.1	829.7
Shared-5	86.3	867.4
Shared-4	86.0	873.8
CoQuiAas	76.2	1477.2
DIAMOND	75.2	1555.4
ArgSemSAT	70.5	1826.6
Conarg	67.8	1976.4
ASGL	57.3	2647.6

System	EE-PR		EE-ST	
	Class.	M-Reg.	Class.	M-Reg.
ArgSemSAT	0	253	0	212
ArgTools	**311**	305	138	428
ASGL	6	36	0	35
ASPARTIX-D	2	80	**305**	409
ASPARTIX-V	1	99		
Cegartix	221	**403**		
Conarg	157	122	231	337
CoQuiAas	43	44	288	193
DIAMOND	0	65	33	138
GRIS	153	278		
LabSATSolver	13	208	228	**548**
prefMaxSAT	297	301		

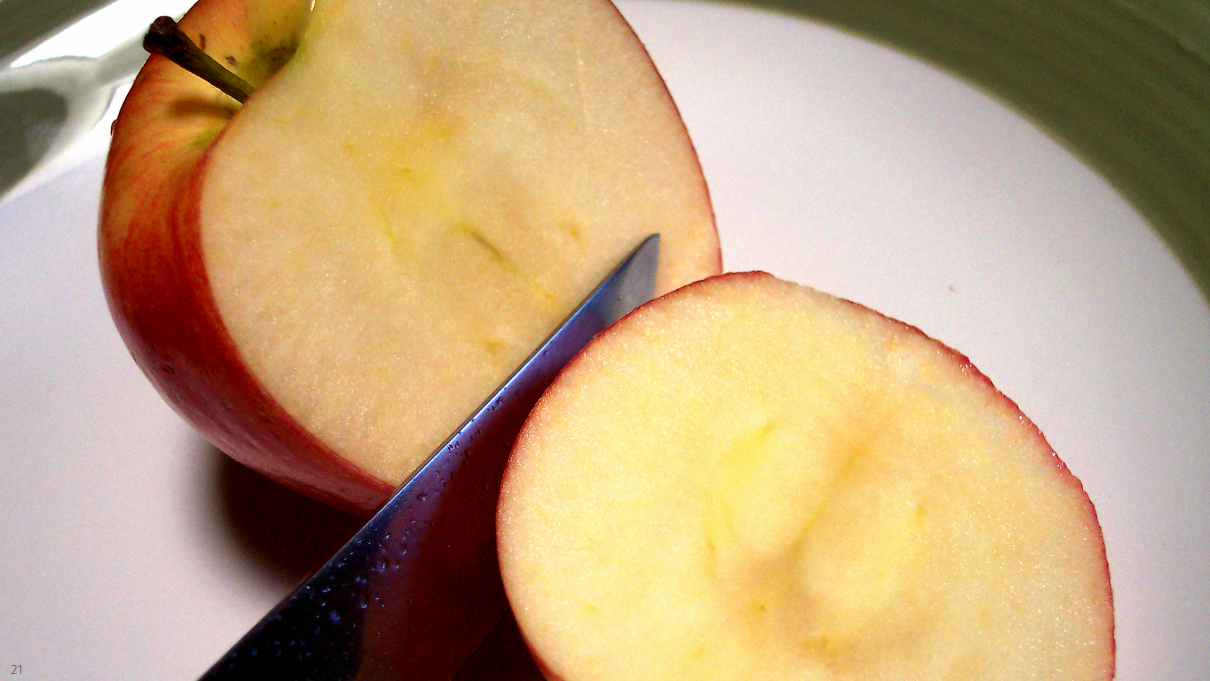

LEAVE-ONE-SET-OUT SCENARIO: PREFERRED EXTENSIONS

	EE-PR							
	Barabasi-Albert		Erdös-Rényi		StableM		Watts-Strogatz	
System	Cov.	PAR10	Cov.	PAR10	Cov.	PAR10	Cov.	PAR10
Classify	**78.9**	**1321.4**	**88.6**	**745.0**	74.4	1574.3	**89.5**	**677.8**
1-Regression	76.3	1479.0	63.0	2255.2	76.5	1453.9	83.0	1079.9
M-Regression	70.4	1828.4	67.3	2039.7	77.0	1434.7	79.6	1267.6
FDSS	69.1	1916.2	80.9	1245.5	**79.1**	**1341.9**	78.6	1380.0
Shared-2	73.2	1678.0	73.2	1678.0	74.2	1620.4	73.2	1678.0
Shared-3	69.4	1892.0	67.3	2007.9	69.5	1896.7	69.4	1892.0
Shared-4	65.7	2106.2	65.7	2101.1	65.7	2108.1	65.7	2103.9
Shared-5	63.3	2240.9	63.4	2235.8	63.3	2242.9	63.3	2242.9

LEAVE-ONE-SET-OUT SCENARIO: STABLE EXTENSIONS

	EE-ST							
	Barabasi-Albert		Erdös-Rényi		StableM		Watts-Strogatz	
System	Cov.	PAR10	Cov.	PAR10	Cov.	PAR10	Cov.	PAR10
1-Regression	88.6	756.9	92.6	508.7	**98.6**	**149.9**	81.6	1153.0
Classify	93.0	470.4	92.4	519.6	91.2	575.6	93.4	439.3
Shared-2	**97.7**	**262.3**	97.3	285.2	97.7	220.9	**97.7**	**262.3**
M-Regression	96.2	297.4	**96.4**	**282.2**	95.6	334.9	90.3	636.5
Shared-3	94.0	420.1	94.0	435.5	94.0	420.1	94.0	476.6
FDSS	89.4	677.4	87.1	829.7	89.4	677.4	88.7	714.7
Shared-4	85.9	878.2	86.0	887.5	86.0	873.8	86.8	833.8
Shared-5	86.3	867.4	86.3	870.8	86.3	862.3	84.3	973.4

CONCLUSIONS

1. It is not always the case that that reduction-based solvers always outperform non reduction-based systems;

2. The solvers at the state of the art show a high level of complementarity (specially those able to deal with EE-PR problems), thus they are suitable to be combined in portfolios;

3. Portfolio systems generally outperform *basic solvers*;

4. If the training instances are representative of testing AFs, the existing set of features is informative for selecting most suitable solvers;

5. Classification-based portfolios show good generalisation performance;

6. Static portfolios are usually the approaches which are less sensitive to different training sets.

- Further investigations in the generalisation capabilities of portfolios performance by considering significantly differently-structured AFs, including complex frameworks generated by real-world scenarios;
- Extend the portfolio methods considering SATZilla like approaches, or more sophisticated model-based techniques;
- Testing portfolio methods also in other complex argumentation problems.


CARDIFF
UNIVERSITY
PRIFYSGOL
CAERDYDD